A Journey in Structure-Based Drug Discovery: From Designed Peptides to Protein Surface Topomimetics as Antibiotic and Antiangiogenic Agents

RUUD P. M. DINGS AND KEVIN H. MAYO*

Department of Biochemistry, Molecular Biology & Biophysics, University of Minnesota, Minneapolis, Minnesota 55455

Received April 6, 2007

ABSTRACT

Most biological events are mediated through molecular interactions by proteins, and because proteins are composed of structural units like helices, β-sheets and turns, small peptides and peptidomimetics may be used to mimic their biological effects and even as therapeutic agents in the clinic. Here, we present a structure-based, scaffold-driven approach to design bioactive peptides and peptidomimetics. Initially, we designed a novel series of β-sheet-forming peptides that mimic the activities of both antibiotic bacterial membrane disrupting peptides and antiangiogenic proteins. We subsequently used structure–activity relationships to reduce the design to partial peptide mimetics and then to fully nonpeptide topomimetics. Some of these agents are currently in extensive preclinical studies for further development as drug candidates against infectious disease and cancer.

Introduction

There are two fundamental paradigms to drug discovery: target-based and activity-based approach. Target-based drug discovery involves identifying compounds that bind specifically to a therapeutic molecular target. Developments in genomics and proteomics have promoted the target-based approach. Prior to the molecular age, activity-based drug discovery, which involves identifying compounds based usually on some in vitro activity assay (and is not limited by ignorance regarding the molecular target), was the standard for lead therapeutic discovery. Ideally, identification of the drug target and mechanism of action would follow during later stages of the drug development process. These two paradigms are not mutually exclusive, and drug discovery can employ a bilateral approach. Using either approach, investigators normally employ high-throughput screening (HTS) of small molecule libraries to identify lead compounds. Somewhere during this process, structure–activity relationships (SAR) among compounds displaying the most potent binding and/or functional activities are developed for use in lead optimization. In some instances, a structural biology (X-ray crystallography or NMR spectroscopy) approach is employed to better understand the molecular level of the target–lead interaction and aid in drug optimization, as perhaps best exemplified with Gleevec (Novartis), where structural knowledge for autoinhibition of c-Abl tyrosine kinase led to an improved pharmaceutical agent.[1]

While HTS has successfully identified some novel drug leads, it provides neither the rate of output nor the number of new drugs previously envisioned. For example, in the year 2000, all existing drugs put together were estimated to hit only about 400 different therapeutic targets, with most potentially novel drugs being missed (as there are at least 10 times more potential drug targets that could be exploited).[2] Moreover, HTS has a low hit rate (about 0.5%). We recently demonstrated that this hit rate can be greatly improved (about 7-fold) by prescreening compound databases using SAR-derived pharmacophore models.[3,4] In this regard, integrating structure-based design into the drug discovery process may hold the key to identifying novel drugs. Here, we present an Account of our structure-based approach to design bioactive peptides and peptidomimetics. These novel pharmaceutical agents have the potential to combat various pathological disorders in the areas of infectious disease and angiogenesis-mediated diseases, e.g., cancer, arthritis, atherosclerosis, restenosis, and endometriosis.

The Journey Begins with the Design of βpep Peptides

Our journey began in the early 1990s with an interest in protein folding of CXC chemokines. One study in particular demonstrated that the 33-residue β-sheet domain of CXC chemokine platelet factor-4 (PF4), independent of the remainder of the sequence, formed native-like β-sheet structure.[5] By comparing folding/solubility parameters on PF4 and other CXC chemokine-derived peptides with those on previously designed β-hairpin peptides (beta-doublet, betabellins) that formed minimal β-sheet structure and displayed limited solubility in aqueous solution,[6] we formulated a recipe to design peptides that would form relatively stable β-sheet structures in aqueous solution and remain soluble under physiological conditions. The success of our recipe rested in the adjustment of the ratio of

Ruud P. M. Dings received his M.S. degree in Biological Health Sciences specializing in tumor vascular immunology, from the University of Maastricht, The Netherlands, in 2000. He received his Ph.D. degree from the same institution in 2003, working jointly in the labs of Prof. Arjan W. Griffioen (Maastricht) and Prof. Kevin H. Mayo (University of Minnesota), studying experimental oncology with special interest in angiogenesis. Presently, he is a research associate in the lab of Prof. Mayo. His research concentrates on drug design and development in infectious diseases and cancer. He is currently on the editorial board of *Angiogenesis*.

Kevin H. Mayo received his A.B. degree in chemistry and biology in 1976 from Boston University and his Ph.D. degree in 1980 from the University of Massachusetts/Amherst under the direction of Prof. James C. W. Chien. Having been awarded an Alexander von Humboldt Fellowship, he worked in the labs of Prof. Rudolf Moessbauer and Prof. Fritz Parak at the Max Planck Institute for Biochemistry and the Technical University of Munich. Following a second postdoctoral stint at Yale University with Prof. James Prestegard, he joined the chemistry faculty at Temple University in 1984 and then moved with Prof. Carlo Croce to Jefferson University, before taking his current position as Professor at the University of Minnesota. His research interests lie generally in structure-based design of peptides and peptidomimetics. He has served on a number of editorial boards and is presently Deputy Chair of the *Biochemical Journal*.

* To whom correspondence should be addressed: Phone 612-625-9968. Fax 612-624-5121. E-mail mayox001@umn.edu.

10.1021/ar700086k CCC: $37.00
Published on Web 07/28/2007

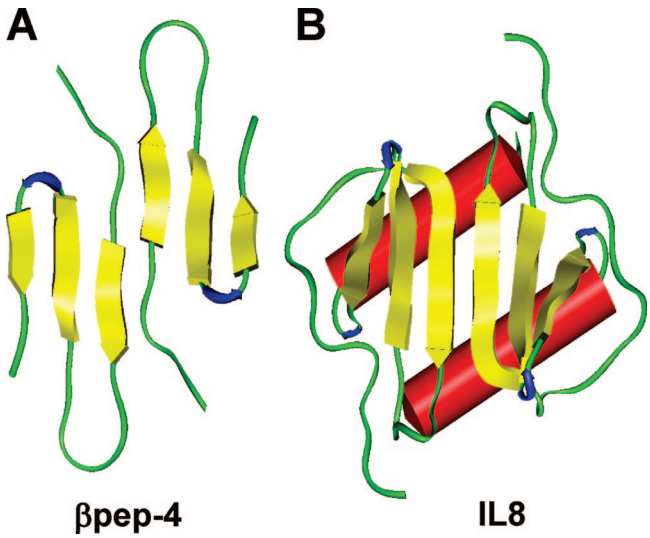

FIGURE 1. Structure of βpep-4 and CXC chemokines. The structures of βpep-4[7] (A) and the CXC chemokine interleukin-8 (IL8)[73] (B) are shown.

certain hydrophobic to hydrophilic residues as well as their appropriate placement within the sequence to optimize desired cross-strand interactions.[6]

Using NMR spectroscopy, we elucidated the solution structure of βpep-4 (Figure 1A) and found that this designed peptide did indeed fold as an antiparallel β-sheet with a similar β-strand arrangement as in native CXC chemokines (e.g., IL8, Figure 1B).[7] Moreover, we observed that βpep-4 monomers can also associate as β-sheet sandwich dimers and tetramers,[7] similar to CXC chemokines. Other βpep peptides also formed relatively stable β-sheet structures in aqueous solution.[6,8]

Antibiotic Activities of *β*pep Peptides. Our foré into drug design began with the discovery that an amino acid sequence from bactericidal/permeability increasing (BPI) protein (residues 82–108) is relatively bactericidal and can neutralize endotoxin lipopolysaccharide (LPS) like parent BPI.[9] Because the homologous amino acid sequence from Limulus Activating LPS Factor (LALF, whose X-ray structure was known at that time,[10] whereas the structure of BPI was solved later[11]) is conformed as a β-sheet/loop, we hypothesized that these activities would increase by stabilizing the β-sheet structure. We modeled in silico BPI peptide 82–108 as a β-sheet based on the X-ray structure of LALF and used our βpep as a β-sheet presentation scaffold to create βpep peptides with appropriately placed residues from BPI peptide 82–108 thought to be responsible for bactericidal and LPS neutralizing activities.[12]

This design effort proceeded iteratively with the goal to optimize activity and eventually led to a library of 30 homologous βpep peptides (βpep-1 to βpep-30), a few of which we found to be more potent that BPI peptide 82–108 and equipotent to native BPI.[13] Because these cationic peptides appear to function by disrupting bacterial membrane integrity, it is less likely that bacterial resistance will be a problem unlike most presently used antibiotics that inhibit function of specific bacterial enzymes or membrane components.[14] We also discovered a potently bactericidal, cationic dodecapeptide, SC4 ($KLFKRHLKWKII\text{-}NH_2$), that folds as an amphipathic helix.[15] These findings led us to conclude that bactericidal activity is more related to the amphipathic and cationic nature of these peptides, as opposed to the specifics of their backbone folds. This structural observation is consistent with other antibiotic peptides reported in the literature.[14]

***β*pep-25 (Anginex) Inhibits Angiogenesis and Tumor Growth.** Angiogenesis, generally defined as the biological process by which new microvasculature is formed from pre-existing blood vessels, is important to normal bodily functions like embryogenesis and wound healing as well as to pathologic disorders like atherosclerosis, restenosis, rheumatoid arthritis, diabetic retinopathy, neovascular glaucoma, and cancer. Because angiogenesis is crucial to many pathologies, investigators have devoted considerable effort to develop agents that either promote or inhibit angiogenesis.[16] Because of our specific interest in cancer, we focused our research efforts on this pathological disorder. Since the development of tumors is dependent upon angiogenesis,[17,18] the inhibition of angiogenesis had been hypothesized as a potentially effective therapeutic approach against tumor growth.[19–21] This has been demonstrated in many animal models and recently in the clinic with, e.g., Avastin (Genentech), Thalomid (Celgene), and Endostar (Medgenn). In fact, it was the clinical success of the VEGF inhibitor Avastin[22] that prompted the pharmaceutical industry to invest considerable effort to generate numerous compounds that interfere with growth factor signaling, e.g., VEGF, FGF, and PDGF. For example, the phage display screening approach has led to identification of a VEGFR2-derived heptapeptide that antagonizes VEGF-VEGFR2 binding,[23] and small molecule HTS and optimization produced a VEGFR2 kinase inhibitor SU5416.[24]

Because most antiangiogenic proteins and peptides (e.g., endostatin, angiostatin, PF4, thrombospondin, gamma interferon-inducible protein-10 (IP-10), tumor necrosis factor, BPI, thrombospondin type 1 repeat peptides, Flt-1 peptide) are structurally and compositionally homologous to βpep peptides (antiparallel β-sheet structure and a preponderance of positively charged and hydrophobic residues),[25] we screened our library of 30 βpep peptides (see preceding section Antibiotic Activities of βpep Peptides) for the ability to inhibit endothelial cell (EC) proliferation, an in vitro indicator of angiogenic potential.[26] We identified βpep-25 (anginex) as a potent angiogenesis inhibitor, more effective than other well-known antiangiogenics, like PF4, IP-10, endostatin, and TNP-470. The sequence of anginex is shown in Figure 2, along with the NMR-derived structure of the peptide.[27] The potency of anginex as an antiangiogenic agent was initially demonstrated in the in vivo chick embryo chorioallantoic membrane (CAM) angiogenesis assay.[26]

Most importantly, anginex inhibits tumor growth by attenuating tumor angiogenesis, as we observed in human colon and ovarian carcinomas in athymic mice[28–32] and murine melamoma and breast sarcomas in syngeneic

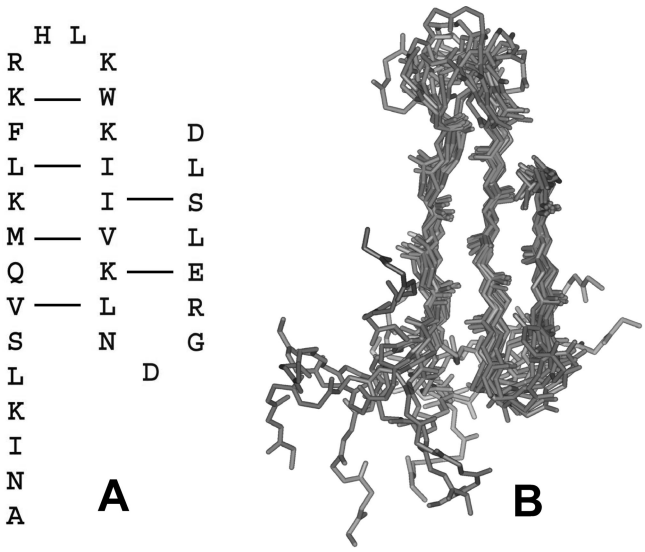

FIGURE 2. Sequence and NMR structure of Anginex (βpep-25). The amino acid sequence of anginex (A) is folded as found in the NMR-derived structure (superposition of 20 calculated structures) of the peptide[27] (B).

mice (e.g., Figure 3A).[28,31–33] Furthermore, anginex showed a very pronounced inhibitory effect on glioma tumors in rats[34] as well as in combination with other antiangiogenics,[30] chemotherapeutics,[30] and radiation[32,33] (e.g., Figure 3B). We also observed that conjugation to a carrier protein (serum albumin) enhanced the ability of anginex to inhibit tumor growth, apparently by improving its in vivo exposure.[29] In general, we found that anginex was most effective against slower growing tumors, and because these better approximate the growth rate of tumors in humans, we suggest that anginex, or one of its mimetics, may have a very good possibility to be effective against cancer in humans.

Mechanistically, we know that anginex inhibits tumor growth in two ways. First, anginex inhibits EC adhesion to and migration on the extracellular matrix which leads EC to apoptosis (a process known as anoikis).[26] Second, anginex promotes leukocyte infiltration (particularly subsets of cytotoxic $CD8^+$ T-cells, polymorphonuclear (PMN) cells, and macrophages) into tumors by normalizing the levels of endothelial adhesion molecule (EAMs, like ICAM, VCAM, and E-selectin) expression that is normally suppressed by tumor-releasing pro-angiogenic compounds like vascular endothelial growth factor (VEGF) and basic fibroblast growth factor (bFGF).[35–37]

Using yeast 2-hybrid screening, we identified the anginex receptor as galectin-1 (gal-1),[38] which belongs to a phylogenetically conserved family of carbohydrate binding lectins (galectins) that share a conserved carbohydrate recognition domain.[39] Gal-1 binds β-galactoside groups on various cell surface receptors and is integral to efficient EC adhesion and migration,[40] particularly to highly proliferative EC within tumors.[38] BIAcore analysis and NMR spectroscopic HSQC chemical shift mapping using purified gal-1 proved that anginex indeed binds gal-1 with a K_d of about 90 nM.[38] The observation that gal-1 does not appear to be involved in normal bodily processes, like

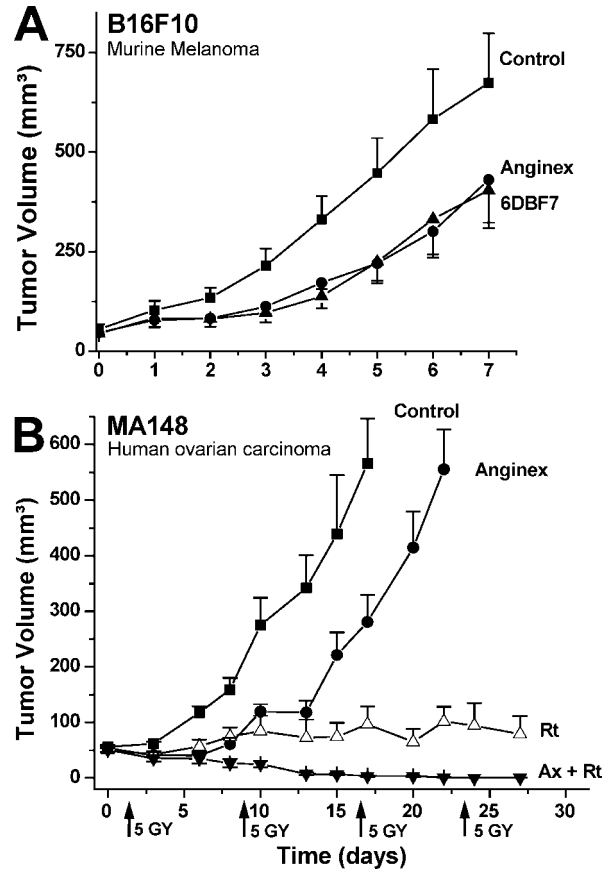

FIGURE 3. Anginex and partial peptide mimetic 6DBF7 inhibit tumor growth in mice. (A) B16F10 melanoma tumor growth is inhibited by anginex and 6DBF7 when administered twice daily by intraperitoneal injections (10 mg/kg). (B) Combination therapy of anginex and radiation leading to MA148 tumor growth reduction. Anginex was administered subcutaneously via osmotic minipumps. Symbols are defined as follows: control ■, anginex (Ax, 10 mg/kg) ●, 6DBF7 (10 mg/kg) ▲, radiation (Rt, 5 Gy q7dx4) △, and combination of Ax and Rt ▼. In all experiments, treatment was initiated after tumors were established. Tumor volumes ($mm^3 \pm$ SEM) are plotted vs days post-inoculation; $n = 10$ in each group for both models.

wound healing,[41] suggests that the increased expression of gal-1 found in human tumors[38] renders the protein an excellent target for therapeutic purposes.

Since gal-1 is crucial to several processes required for tumor growth, this may explain why anginex (and its mimetics) displays multimodal activities (inhibition of EC proliferation and promotion of leukocyte infiltration into tumors). For instance, interfering with gal-1 function could (i) prevent tumor angiogenesis,[38] (ii) abrogate tumor escape from immunity through blockade of gal-1-induced apoptosis in activated T lymphocytes,[42] and (iii) prevent metastasis formation through inhibition of gal-1 facilitated tumor cell–EC interactions.[43] Aside from targeting gal-1, anginex has also been shown to interact weakly and seemingly nonspecifically with plasma fibronectin.[44] Because of this observation, we propose that the function of fibronectin is to carry anginex through the vascular network to the site of angiogenic activity, and thereby via mass action, to better promote interaction of anginex with its target, gal-1.

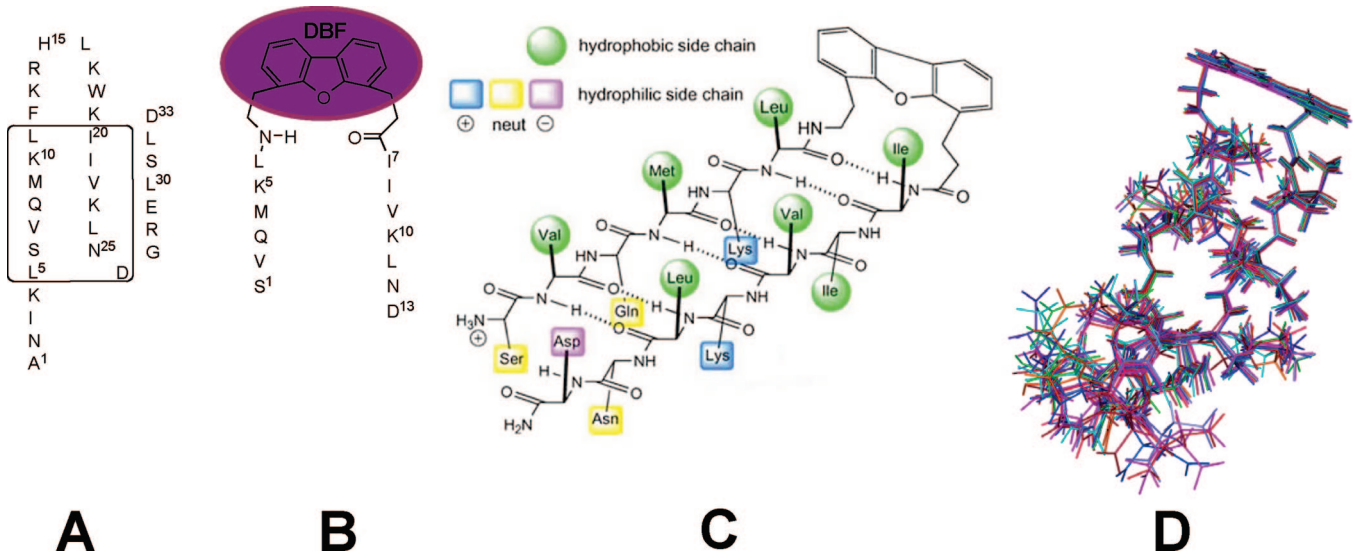

FIGURE 4. Design of the dibenzofuran (DBF) mimetics. The amino acid sequence of anginex is shown with functionally important residues boxed (A), next to compound 6DBF7 with its dibenzofuran (DBF) scaffold highlighted (B). A depiction of 6DBF7 is shown with the DBF moiety canted to illustrate interaction of the Leu and Ile residues with the aromatic groups of DBF (C). The NMR-derived superimposed structures of 6DBF7[56] are shown in (D).

A number of other antiangiogenics are known to function by inhibiting EC adhesion and/or migration. The most notable are those mimicking the fibronectin-derived RGD tripeptide that targets integrins,[45] e.g., antagonizing integrins $\alpha_2\beta_3$ and $\alpha_V\beta_5$.[46] RGD-based strategies have also been used for the delivery of therapeutics and imaging to tumor vasculature.[47] Other examples of adhesion/migration antagonizers are thrombospondin-1 (TSP-1)-derived peptides[48] and TSP-1 nonamer mimetic ABT-510,[49] extracellular matrix laminin α1 chain-derived peptides AG73 and EF-1 that bind to syndecan and integrin $\alpha_2\beta_1$,[50,51] and an N-terminal peptide derived from endostatin, ES-2, that targets β1-integrin.[52]

Anginex as a Tumor Targeting Device. Recently, we also showed that anginex can be used as a tumor targeting or homing device. By chemically coupling anginex through a C-terminal cysteine to lipid vesicles, we found, using magnetic resonance imaging, that anginex concentrated in vessels at the site of the tumor.[53] We are currently optimizing the utilization of anginex-coupled vesicles to deliver chemotherapeutic and contrast agents loaded within the vesicles to treat and image tumors, respectively.[53–55]

Dibenzofuran-Scaffolded Partial-Peptide Mimetics of Anginex

Having demonstrated the potential of anginex as an antiangiogenic and antitumor agent, we focused our efforts on reducing its molecular size and peptidic nature. We first performed structure–activity relationship (SAR) studies on anginex to identify residues responsible for angiostatic activity. By assessing the ability of alanine scanning analogues of anginex to inhibit EC proliferation, we demonstrated that several hydrophobic residues within the first two β-strands were most important to promote the activity of anginex.[56] Functionally important hydrophobic residues were found to occur at alternating positions (i, $i + 2$), consistent with a β-strand motif, as well as at cross-strand positions that comprise the hydrophobic face of the amphipathic β-sheet structure (Figure 4A, key residues boxed). We also found that positive charge character was important to angiostatic activity.[56]

Although NMR-derived structures of βpeps,[7,27] in combination with these SAR studies, strongly suggested the importance of β-sheet structure to activity, we used cysteine-substituted, disulfide-linked analogues of anginex to firmly establish that antiparallel β-sheet defines the bioactive conformation.[57] Moreover, when the disulfide bond linkage was not positioned to align β-strands as shown in Figure 2A, angiostatic activity all but vanished, demonstrating the requirement for this specific alignment of the β-strands.[57]

Because our SAR studies showed that C-terminal residues G27-D33 and the loop (R12-W19) between β-strands 1 and 2 were dispensable,[56] we designed a partial peptide mimetic of anginex that contained the remnants of β-strands 1 and 2 (key amino acids boxed in the structure of anginex shown in Figure 4A) and a β-turn mimetic scaffold to induce β-sheet formation. From a number of such scaffolds,[58] we selected dibenzofuran (**DBF**, Figure 4B).[59] When **DBF** is inserted between a pair of lipophilic residues (e.g., I20 and L11 of anginex, Figure 4A), a "hydrophobic cluster" is created wherein the side chains of those residues are nested within the hydrophobic pocket created by the aromatic rings of the canted **DBF** subunit (Figure 4C).

With this in mind, we first produced the **#DBF7** series of compounds, where the numbers at the left and right of the **DBF** give the number of residues at the N-terminus and C-terminus, respectively, with the **DBF** scaffold at the center (Figure 4B). In this series of **DBF** analogs, the seven amino acid residues on β-strand 2 were maintained due to the importance of that sequence. We elucidated the

NMR solution structure of **6DBF7** (Figure 4D)[56] and demonstrated that it maintained a β-sheet fold, as envisioned in Figure 4C. The general topology of these **DBF** scaffolded β-sheet structures has an alternating sequence of nonpolar vs polar amino acid residues, as in anginex, which results in one face of the sheet being adorned largely with hydrophobic substituents and the other face with largely positively charged, neutral, and hydrophilic negatively charged (Figure 4C,D).

Using EC proliferation, migration, and sprouting assays, we found that of these **DBF** analogues **6DBF7** displayed the greatest antiangiogenic activity with, e.g., an IC_{50} of 15 μM in the EC proliferation assay compared to 4 μM for parent anginex.[56] In vivo however, **6DBF7** was at least equipotent to, or better than, anginex. In the MA148 ovarian carcinoma model, **6DBF7** inhibited both tumor growth and tumor angiogenesis about 2-fold better than anginex,[56] whereas in the murine B16F10 melanoma model, their activities were equivalent (e.g., Figure 3A). In these in vivo experiments, no apparent sign of general toxicity from **6DBF7** or anginex was observed, as assessed by unaltered behavior and normal weight gain of the animals, and no change in hematocrit and creatinine levels in the blood. Moreover, macro- and microscopic morphology of internal organs were also observed to be normal within all experimental groups of animals.

The following section describes the next logical step, where we designed a series of nonpeptidic agents that mimic the amphipathic nature of anginex and **6DBF7** and exhibit antiangiogenic and antibacterial activities.

Protein Surface Topomimetics

Interactions among biomolecules dictate biological events. For optimal activity, these interactions should be complementary in terms of their surface topology and chemical composition, as illustrated e.g. in Figure 5. With proteins, the interaction surface is defined by the spatial arrangement of amino acid side chains (i.e., chemical groups) that are scaffolded in place by the peptide backbone (e.g., Figure 5), which by itself is usually irrelevant (with the noted exception of enzyme active sites) to the interaction surface. By using an organic scaffold with appropriate chemical appendages to mimic the molecular dimensions, surface topology, and chemical composition of structural units (β-sheets or hairpins and helices) that comprise at least part of any protein interaction surface, we have at hand a paradigm to guide the design of nonpeptidic molecules that can interfere with (usually antagonize) protein-mediated biomolecular interactions. This concept forms the basis for the design of our protein surface topomimetics, and although the general idea to design peptidomimetics has been around for some time, our topomimetic design approach has been most successful, as will be evident in the following sections.

Protein Surface Topomimetics Using Calix[4]arene as the Scaffold. For proof of concept of our topomimetic design paradigm outlined above, we used two of our designed amphipathic peptides as models: the antiparallel

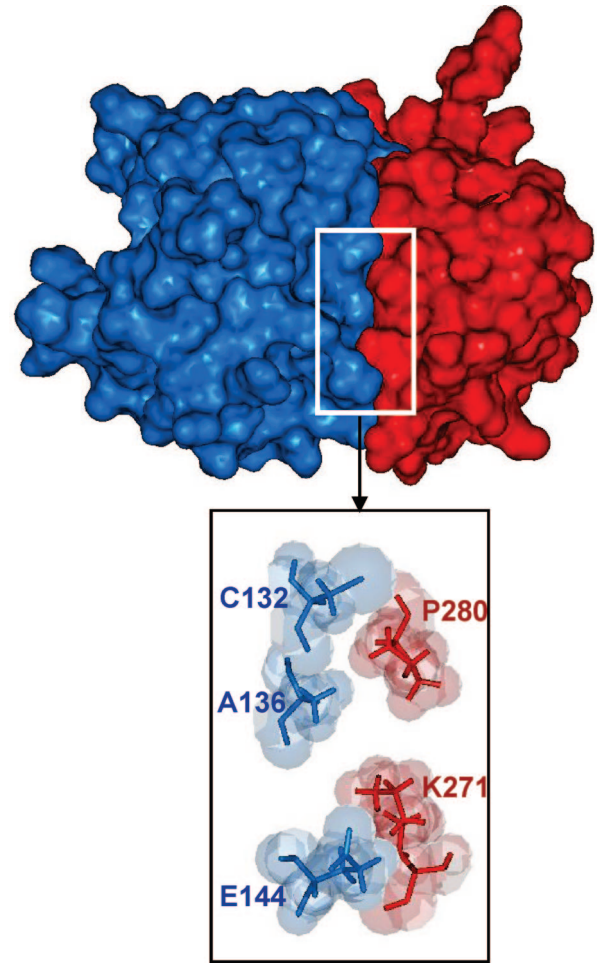

FIGURE 5. Illustration of a protein–protein interaction surface. A space-filling model of the structure of the eIF4G/eIF4E protein–protein complex is shown[74] along with an expansion of the interface between the two proteins to indicate a few residue to residue contacts. Mimicking either side of this interface could produce an antagonist to inhibit the interaction.

β-sheet anginex and helical SC4. Figure 6A illustrates our design concept using the calix[4]arene scaffold. The structural unit encompassing key residues in anginex covers approximately the dimensions of a two-stranded β-sheet only about four amino acid residues in length on each strand, while that in SC4 covers approximately the dimensions of two turns of helix. In both cases, the overall backbone dimensions are similar to those of a calix[4]arene scaffold (Figure 6A). Adding hydrophobic and basic chemical groups to the calix[4]arene scaffold can increase the molecular surface span on each side of the scaffold up to about 15 Å, which approximates maximal distances between proximal side chains in a β-sheet or helix. From structural biology and synthetic chemistry perspectives, calixarene provided a very good scaffold from which to position chemical groups that mimic the character and surface topology of key amino acid side chains in anginex and SC4. On the basis of this rationale, we synthesized a relatively small library of 23 calixarene-based compounds, with each analogue displaying chemical substituents to mimic the approximate molecular dimensions and am-

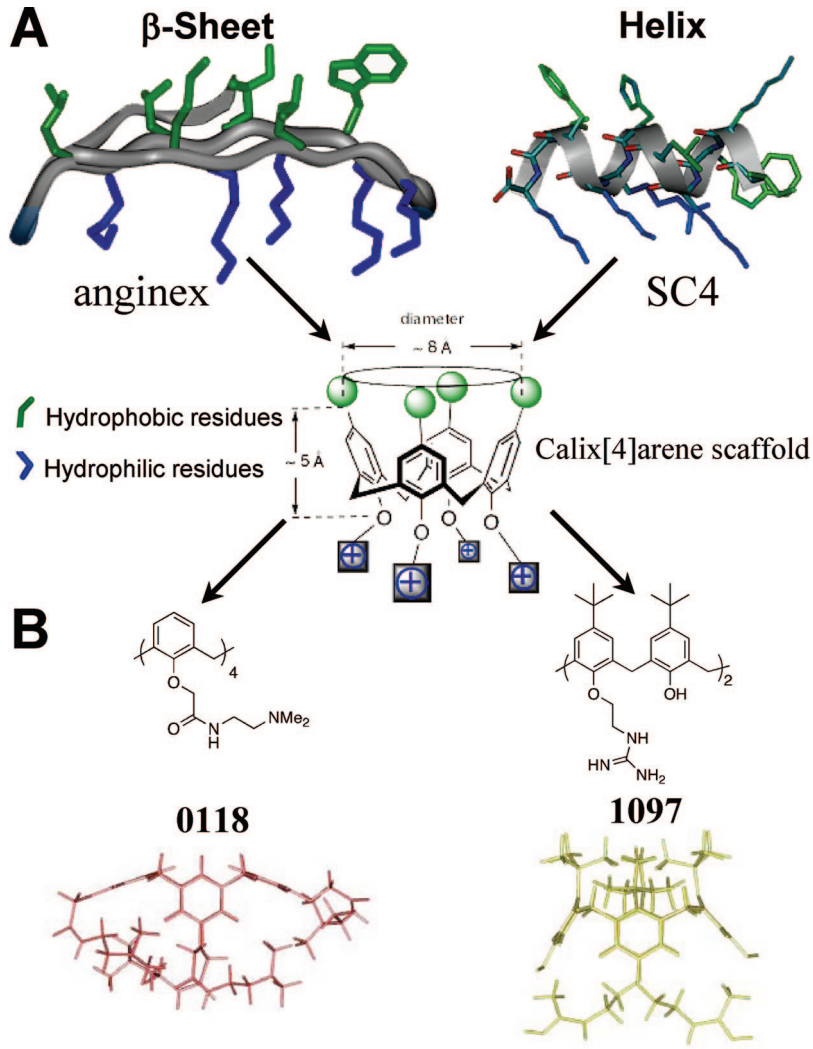

FIGURE 6. Design of calixarene-based topomimetics. (A) The NMR-derived structures of anginex[27] and SC4[15] peptides are shown, essentially to scale with the calix[4]arene scaffold. (B) The chemical and in silico energy-minimized structures of two calixarene analogues, 0118 and 1097,[31] which mimic the molecular dimensions and chemical compositions of either peptide, are shown at the bottom of the figure.

phipathic features of folded anginex and SC4 (Figure 6A). Nearly all could be prepared rather easily via a four to six step long synthetic route, with a yield of multi-ten milligram quantities.

Our "small molecule" library of calixarene compounds is quite unique because these calixarene-based protein surface topomimetics maintain volume like that found in a small segment of β-sheet, β-hairpin, or helix that displays more of the entire surface of these segments. This distinguishes them from other calixarene-scaffolded compounds that merely display peptide fragments derived from VEGF and PDGF to inhibit angiogenesis.[60–62] Other peptidomimetics reported in the literature generally consist of short peptide-like sequences that are constrained[63,64] or use nonnatural amino acid residues,[65] or they consist of what we would call "linear two-dimensional" organic molecules that contain chemical groups to mimic amino acid side chains.[66–71] Such "traditional" compounds comprise most "small molecule" libraries; however, as far as drug discovery is concerned, a chemical library is only as good as the breadth and variety of the compounds in it. In this respect, we would expect members from our calixarene library to perhaps hit novel targets not normally probed by the conformational space represented with compounds in traditional libraries.

Inhibition of Angiogenesis and Tumor Growth in Vivo. Since the molecular target of anginex was unknown at the time we created this topomimetic library, we used the activity-based approach to screen for antiangiogenic activity on the hypothesis that a topomimetic of anginex could elicit similar biological responses. Moreover, because many antiangiogenic proteins consist primarily of β-sheet structure with significant hydrophobic and cationic character like anginex,[25] we felt that even if we did not "hit" the same target as anginex, we could discover compounds with antiangiogenic activity.

Using the EC proliferation assay, we screened the topomimetic library and identified two members **0118** and **1097** (Figure 6B) to be potent inhibitors of EC growth.[31] Topomimetic **0118** ($IC_{50} = 2\ \mu M$) was slightly more active than anginex ($IC_{50} = 4\ \mu M$) and considerably more active than **1097** ($IC_{50} = 8\ \mu M$). Because both topomimetics also retarded EC migration,[31] we speculated that both topomimetics would very likely be angiostatic in vivo as well.

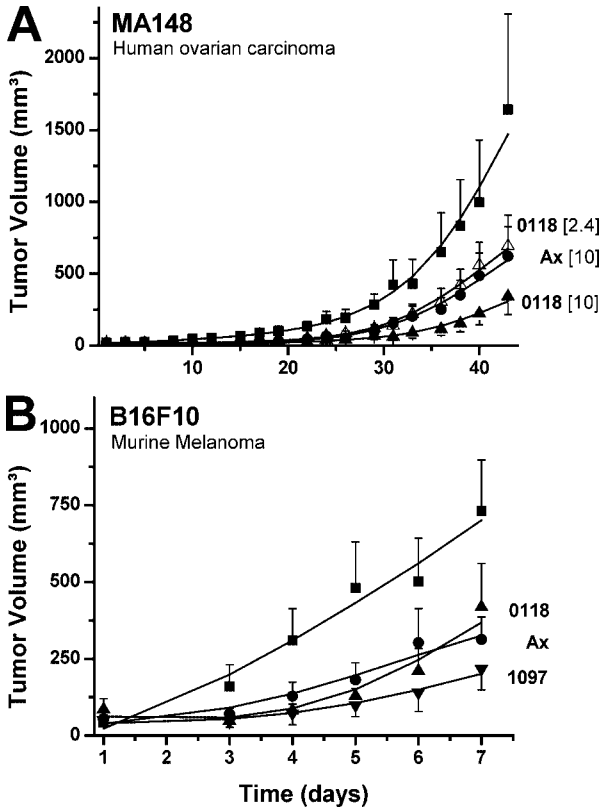

FIGURE 7. Topomimetics inhibit tumor growth in mice. (A) MA148 tumor bearing mice were treated with anginex (10 mg/kg/day) as well as with pharmacological (10 mg/(kg day)) and molar equivalent (2.4 mg/(kg day)) doses of 0118. Compounds were administered via osmotic minipumps. (B) B16F10 melanoma tumor growth is inhibited by 0118 and 1097 administered twice daily by intraperitoneal injections for a total dose of 10 mg/(kg day). In all studies, treatment was initiated after tumors were established. Tumor volumes (mm^3 ± SEM) are plotted vs days post-inoculation. For the MA148 model, $n = 5$–7 mice in each group; for the B16 model, $n = 6$–10 in each group. All treatment groups inhibited tumor growth significantly compared to control treated mice ($p = 0.001$ using the two-way ANOVA analysis). In all panels, symbols are defined as: control ■, anginex (Ax, 10 mg/kg) ●, 0118 (2.4 mg/kg) △, 0118 (10 mg/kg) ▲, and 1097 (10 mg/kg) ▼.

We first demonstrated this using the chorioallantoic membrane (CAM) assay in fertilized chicken eggs, where both **0118** and **1097** significantly inhibited angiogenesis,[31] like anginex.[26]

We subsequently assessed the in vivo efficacy of **0118** and **1097** in two tumor growth models (ovarian carcinoma and melanoma) in mice (Figure 7A,B).[28–32] In the human ovarian carcinoma model, tumor growth (compared to untreated controls) was significantly inhibited, more so when mice were treated (10 mg/kg dose) with topomimetic **0118** (about 80% inhibition, Figure 7A) than with **1097** (about 65% inhibition, data not shown). However, in the murine B16F10 melanoma model, **1097** was slightly more efficacious than **0118** (Figure 7B). These in vivo activities from topomimetics **0118** and **1097** were slightly greater than from anginex, as discussed above.[31] Angiostatic potential in vivo was demonstrated immunohistochemically to identify blood vessels by using fluorescently labeled anti-CD31 antibodies to stain cross sections of tumor tissue. We observed that both **0118** and **1097** significantly diminished vessel density and modified vessel architecture in tumors from treated animals.[31] Moreover, treatment with **0118** and **1097** also increased the rate of tumor cell apoptosis.[31]

In all in vivo experiments, we did not see signs of general toxicity from **0118** or **1097**, as assessed in the animals by unaltered behavior, normal weight gain, and hematocrit and creatinine levels in the blood. Moreover, macro- and microscopic morphology of internal organs were also observed to be normal within all experimental groups of animals.

Lastly, while topomimetics **0118** and **1097** are potently antiangiogenic and inhibit tumor growth, we presently do not know for sure whether either compound also targets the anginex receptor, galectin-1. However, two pieces of evidence suggest that **0118** may be a true mimetic of anginex: (1) compound **0118** functions both in vitro and in vivo just like anginex and (2) preliminary NMR data from HSQC chemical shift mapping using purified gal-1 indicate that **0118** does interact with gal-1 at the same site as anginex (unpublished data). On the other hand, we feel confident that **1097** operates via a different target, albeit also involved in EC adhesion and migration.

Topomimetics Neutralize LPS and Kill Bacteria. Because there is a structure–function relationship between antiangiogenic and bactericidal peptides,[25,31,72] we tested our calixarene-based topomimetics for the ability to kill bacteria and to neutralize LPS endotoxin. Several of these compounds exhibit minimal inhibitory concentration (MIC) values in the single digit micromolar range, and at least two of them increase survival of mice challenged directly with log phase growth bacteria (unpublished data). In terms of neutralizing LPS, some of the topomimetics are as effective as BPI and polymyxin B (IC_{50} in the 10^{-8} M range). Moreover, in an endotoxemia mouse model, three of them are at least partially protective against direct challenges with LPS.[72] Mechanistically, NMR studies indicate that these topomimetics interact with the lipid A component of LPS, with binding being mediated by electrostatic and hydrophobic interactions.[72]

Concluding Remarks and Future Directions

We reported here an account of our structure-based design from βpep peptides and partial peptide mimetics on the discovery of promising new protein surface topomimetics for clinical intervention against infectious disease and cancer and angiogenesis-mediated diseases in general. Our protein surface topomimetics expand the flavor of compounds presently found in small molecule and peptidomimetic libraries and, by their novel nature, may hold the key to identify new targets not normally probed by the chemical character and/or conformational space represented by compounds in traditional chemical libraries. Our topomimetic design may have broad applications to various other physiological processes and pathological disorders, as these protein surface topomimetics may be used to antagonize other protein–

biomolecular interactions. For example, we can readily modify the composition and chemical character of either or both surfaces (hydrophilic/hydrophobic) in our calixarene-based topomimetics. In fact, we have already successfully accomplished this in a few different systems to be reported in future publications.

The research that we described in this Account could only have been achieved through the combined and complementary scientific expertise from the labs of our collaborators. Therefore, the authors are most grateful to Prof. Thomas Hoye and Prof. Arjan Griffioen. We also thank Ms. Michelle Miller and Dr. Irina Nesmelova for assistance in producing some of the figures shown here. In addition, we acknowledge research support from the National Institutes of Health (NIAID grant AI-057153 and NCI grant CA-096090).

References

(1) Nagar, B.; Hantschel, O.; Young, M. A.; Scheffzek, K.; Veach, D.; Bornmann, W.; Clarkson, B.; Superti-Furga, G.; Kuriyan, J. Structural basis for the autoinhibition of c-Abl tyrosine kinase. *Cell* **2003**, *112*, 859–871.

(2) Drews, J. Drug discovery: a historical perspective. *Science* **2000**, *287*, 1960–1964.

(3) Orsini, M. J.; Nesmelova, I.; Young, H. C.; Hargittai, B.; Beavers, M. P.; Liu, J.; Connolly, P. J.; Middleton, S. A.; Mayo, K. H. The nociceptin pharmacophore site for opioid receptor binding derived from the NMR structure and bioactivity relationships. *J. Biol. Chem.* **2005**, *280*, 8134–8142.

(4) Orsini, M. J.; Klein, M. A.; Beavers, M. P.; Connolly, P. J.; Middleton, S. A.; Mayo, K. H. Metastin (KiSS-1) mimetics identified from peptide structure-activity relationship-derived pharmacophores and directed small molecule database screening. *J. Med. Chem.* **2007**, *50*, 462–471.

(5) Ilyina, E.; Mayo, K. H. Multiple native-like conformations trapped via self-association-induced hydrophobic collapse of the 33-residue beta-sheet domain from platelet factor 4. *Biochem. J.* **1995**, *306*, 407–419.

(6) Mayo, K. H.; Ilyina, E.; Park, H. A recipe for designing water-soluble, beta-sheet-forming peptides. *Protein Sci.* **1996**, *5*, 1301–1315.

(7) Ilyina, E.; Roongta, V.; Mayo, K. H. NMR structure of a de novo designed, peptide 33mer with two distinct, compact beta-sheet folds. *Biochemistry* **1997**, *36*, 5245–5250.

(8) Cox, A.; Arroyo, M. M.; Mayo, K. H. Folding of beta pep-4 beta-sheet sandwich dimers and tetramers is influenced by aliphatic hydrophobic residues at the intersubunit interface. *Biochem. J.* **2001**, *357*, 739–747.

(9) Gray, B. H.; Haseman, J. R.; Mayo, K. H. B/PI-derived synthetic peptides: synergistic effects in tethered bactericidal and endotoxin neutralizing peptides. *Biochem. Biophys. Acta* **1995**, *1244*, 185–190.

(10) Hoess, A.; Watson, S.; Siber, G. R.; Liddington, R. Crystal structure of an endotoxin-neutralizing protein from the horseshoe crab, Limulus anti-LPS factor, at 1.5 A resolution. *EMBO J.* **1993**, *12*, 3351–3356.

(11) Beamer, L. J.; Carroll, S. F.; Eisenberg, D. Crystal structure of human BPI and two bound phospholipids at 2.4 angstrom resolution. *Science* **1997**, *276*, 1861–1864.

(12) Mayo, K. H.; Haseman, J.; Ilyina, E.; Gray, B. Designed beta-sheet-forming peptide 33mers with potent human bactericidal/permeability increasing protein-like bactericidal and endotoxin neutralizing activities. *Biochim. Biophys. Acta* **1998**, *1425*, 81–92.

(13) Mayo, K. H.; Haseman, J. R.; Ilyina, E.; Gray, B. Designed beta-sheet-forming peptide 33mers with potent human bactericidal/permeability increasing protein-like bactericidal and endotoxin neutralizing activities. *Biochem. Biophys. Acta* **1998**, *1425*, 81–92.

(14) Lockwood, N. A.; Mayo, K. H. The future of antibiotics: bacterial membrane disintegrators. *Drugs Future* **2003**, *28*, 911–923.

(15) Mayo, K. H.; Haseman, J.; Young, H. C.; Mayo, J. W. Structure-function relationships in novel peptide dodecamerswith broad-spectrum bactericidal and endotoxin-neutralizing activities. *Biochem. J.* **2000**, *349*, 717–728.

(16) D'Andrea, L. D.; Del Gatto, A.; Pedone, C.; Benedetti, E. Peptide-based molecules in angiogenesis. *Chem. Biol. Drug Des.* **2006**, *67*, 115–126.

(17) Folkman, J. Tumor angiogenesis: therapeutic implications. *N. Engl. J. Med.* **1971**, *285*, 1182–1186.

(18) Folkman, J. The role of angiogenesis in tumor growth. *Semin. Cancer Biol.* **1992**, *3*, 65–71.

(19) Boehm, T.; Folkman, J.; Browder, T.; O'Reilly, M. S. Antiangiogenic therapy of experimental cancer does not induce acquired drug resistance. *Nature (London)* **1997**, *390*, 404–407.

(20) O'Reilly, M. S.; Holmgren, L.; Shing, Y.; Chen, C.; Rosenthal, R. A.; Moses, M.; Lane, W. S.; Cao, Y.; Sage, E. H.; Folkman, J. Angiostatin: a novel angiogenesis inhibitor that mediates the suppression of metastases by a Lewis lung carcinoma. *Cell* **1994**, *79*, 315–328.

(21) O'Reilly, M. S.; Boehm, T.; Shing, Y.; Fukai, N.; Vasios, G.; Lane, W. S.; Flynn, E.; Birkhead, J. R.; Olsen, B. R.; Folkman, J. Endostatin: an endogenous inhibitor of angiogenesis and tumor growth. *Cell* **1997**, *88*, 277–285.

(22) Griffin, R. J.; Molema, G.; Dings, R. P. Angiogenesis treatment, new concepts on the horizon. *Angiogenesis* **2006**, *9*, 67–72.

(23) Starzec, A.; Vassy, R.; Martin, A.; Lecouvey, M.; Di Benedetto, M.; Crepin, M.; Perret, G. Y. Antiangiogenic and antitumor activities of peptide inhibiting the vascular endothelial growth factor binding to neuropilin-1. *Life Sci.* **2006**, *79*, 2370–2381.

(24) Fong, T. A.; Shawver, L. K.; Sun, L.; Tang, C.; App, H.; Powell, T. J.; Kim, Y. H.; Schreck, R.; Wang, X.; Risau, W.; Ullrich, A.; Hirth, K. P.; McMahon, G. SU5416 is a potent and selective inhibitor of the vascular endothelial growth factor receptor (Flk-1/KDR) that inhibits tyrosine kinase catalysis, tumor vascularization, and growth of multiple tumor types. *Cancer Res.* **1999**, *59*, 99–106.

(25) Dings, R. P.; Nesmelova, I.; Griffioen, A. W.; Mayo, K. H. Discovery and development of anti-angiogenic peptides: A structural link. *Angiogenesis* **2003**, *6*, 83–91.

(26) Griffioen, A. W.; van der Schaft, D. W.; Barendsz-Janson, A. F.; Cox, A.; Struijker Boudier, H. A.; Hillen, H. F.; Mayo, K. H. Anginex, a designed peptide that inhibits angiogenesis. *Biochem J.* **2001**, *354*, 233–242.

(27) Arroyo, M. M.; Mayo, K. H. NMR solution structure of the angiostatic peptide anginex. *Biochem. Biophys. Acta,* in press.

(28) van der Schaft, D. W.; Dings, R. P.; de Lussanet, Q. G.; van Eijk, L. I.; Nap, A. W.; Beets-Tan, R. G.; Bouma-Ter Steege, J. C.; Wagstaff, J.; Mayo, K. H.; Griffioen, A. W. The designer anti-angiogenic peptide anginex targets tumor endothelial cells and inhibits tumor growth in animal models. *FASEB J.* **2002**, *16*, 1991–1993.

(29) Dings, R. P.; van der Schaft, D. W.; Hargittai, B.; Haseman, J.; Griffioen, A. W.; Mayo, K. H. Anti-tumor activity of the novel angiogenesis inhibitor anginex. *Cancer Lett.* **2003**, *194*, 55–66.

(30) Dings, R. P.; Yokoyama, Y.; Ramakrishnan, S.; Griffioen, A. W.; Mayo, K. H. The designed angiostatic peptide anginex synergistically improves chemotherapy and antiangiogenesis therapy with angiostatin. *Cancer Res.* **2003**, *63*, 382–385.

(31) Dings, R. P.; Chen, X.; Hellebrekers, D. M.; van Eijk, L. I.; Zhang, Y.; Hoye, T. R.; Griffioen, A. W.; Mayo, K. H. Design of nonpeptidic topomimetics of antiangiogenic proteins with antitumor activities. *J. Natl. Cancer Inst.* **2006**, *98*, 932–936.

(32) Dings, R. P.; Loren, M.; Heun, H.; McNiel, E.; Griffioen, A. W.; Mayo, K. H.; Griffin, R. J. Scheduling of radiation with angiogenesis inhibitors Anginex and Avastin improves therapeutic outcome via vessel normalization. *Clin. Cancer Res.* **2007**, *13*, 3395–3402.

(33) Dings, R. P.; Williams, B. W.; Song, C. W.; Griffioen, A. W.; Mayo, K. H.; Griffin, R. J. Anginex synergizes with radiation therapy to inhibit tumor growth by radiosensitizing endothelial cells. *Int. J. Cancer* **2005**, *115*, 312–319.

(34) Mayo, K. H.; Griffioen, A. W. Designing βpep Peptides: A Rational Approach to Discovery of Novel Pharmaceutical Agents and Small Molecules. *Drugs Future* **2003**, 337–346.

(35) Griffioen, A. W.; Damen, C. A.; Blijham, G. H.; Groenewegen, G. Tumor angiogenesis is accompanied by a decreased inflammatory response of tumor-associated endothelium. *Blood* **1996**, *88*, 667–673.

(36) Tromp, S. C.; oude Egbrink, M. G.; Dings, R. P.; van Velzen, S.; Slaaf, D. W.; Hillen, H. F.; Tangelder, G. J.; Reneman, R. S.; Griffioen, A. W. Tumor angiogenesis factors reduce leukocyte adhesion in vivo. *Int. Immunol.* **2000**, *12*, 671–676.

(37) Dirkx, A. E.; oude Egbrink, M. G.; Castermans, K.; van der Schaft, D. W.; Thijssen, V. L.; Dings, R. P.; Kwee, L.; Mayo, K. H.; Wagstaff, J.; Bouma-ter Steege, J. C.; Griffioen, A. W. Anti-angiogenesis therapy can overcome endothelial cell anergy and promote leukocyte-endothelium interactions and infiltration in tumors. *FASEB J.* **2006**, *20*, 621–630.

(38) Thijssen, V. L.; Postel, R.; Brandwijk, R. J.; Dings, R. P.; Nesmelova, I.; Satijn, S.; Verhofstad, N.; Nakabeppu, Y.; Baum, L. G.; Bakkers, J.; Mayo, K. H.; Poirier, F.; Griffioen, A. W. Galectin-1 is essential in tumor angiogenesis and is a target for antiangiogenesis therapy. *Proc. Natl. Acad. Sci. U.S.A.* **2006**, *103*, 15975–15980.

(39) Barondes, S. H.; Castronovo, V.; Cooper, D. N.; Cummings, R. D.; Drickamer, K.; Feizi, T.; Gitt, M. A.; Hirabayashi, J.; Hughes, C.; Kasai, K. Galectins: a family of animal beta-galactoside-binding lectins. *Cell* **1994**, *76*, 597–598.
(40) Rabinovich, G. A. Galectin-1 as a potential cancer target. *Br. J. Cancer* **2005**, *92*, 1188–1192.
(41) Cao, Z.; Said, N.; Amin, S.; Wu, H. K.; Bruce, A.; Garate, M.; Hsu, D. K.; Kuwabara, I.; Liu, F. T.; Panjwani, N. Galectins-3 and -7, but not galectin-1, play a role in re-epithelialization of wounds. *J. Biol. Chem.* **2002**, *277*, 42299–42305.
(42) Rubinstein, N.; Alvarez, M.; Zwirner, N. W.; Toscano, M. A.; Ilarregui, J. M.; Bravo, A.; Mordoh, J.; Fainboim, L.; Podhajcer, O. L.; Rabinovich, G. A. Targeted inhibition of galectin-1 gene expression in tumor cells results in heightened T cell-mediated rejection; A potential mechanism of tumor-immune privilege. *Cancer Cells* **2004**, *5*, 241–251.
(43) Lotan, R.; Matsushita, Y.; Ohannesian, D.; Carralero, D.; Ota, D. M.; Cleary, K. R.; Nicolson, G. L.; Irimura, T. Lactose-binding lectin expression in human colorectal carcinomas. Relation to tumor progression. *Carbohydr. Res.* **1991**, *213*, 47–57.
(44) Akerman, M. E.; Pilch, J.; Peters, D.; Ruoslahti, E. Angiostatic peptides use plasma fibronectin to home to angiogenic vasculature. *Proc. Natl. Acad. Sci. U.S.A.* **2005**, *102*, 2040–2045.
(45) Gentilucci, L.; Cardillo, G.; Squassabia, F.; Tolomelli, A.; Spampinato, S.; Sparta, A.; Baiula, M. Inhibition of cancer cell adhesion by heterochiral Pro-containing RGD mimetics. *Bioorg. Med. Chem. Lett.,* in press.
(46) Maubant, S.; Saint-Dizier, D.; Boutillon, M.; Perron-Sierra, F.; Casara, P. J.; Hickman, J. A.; Tucker, G. C.; Van Obberghen-Schilling, E. Blockade of alpha v beta3 and alpha v beta5 integrins by RGD mimetics induces anoikis and not integrin-mediated death in human endothelial cells. *Blood* **2006**, *108*, 3035–3044.
(47) Temming, K.; Schiffelers, R. M.; Molema, G.; Kok, R. J. RGD-based strategies for selective delivery of therapeutics and imaging agents to the tumour vasculature. *Drug Resist. Updates* **2005**, *8*, 381–402.
(48) Reiher, F. K.; Volpert, O. V.; Jimenez, B.; Crawford, S. E.; Dinney, C. P.; Henkin, J.; Haviv, F.; Bouck, N. P.; Campbell, S. C. Inhibition of tumor growth by systemic treatment with thrombospondin-1 peptide mimetics. *Int. J. Cancer* **2002**, *98*, 682–689.
(49) Markovic, S. N.; Suman, V. J.; Rao, R. A.; Ingle, J. N.; Kaur, J. S.; Erickson, L. A.; Pitot, H. C.; Croghan, G. A.; McWilliams, R. R.; Merchan, J.; Kottschade, L. A.; Nevala, W. K.; Uhl, C. B.; Allred, J.; Creagan, E. T. A phase II study of ABT-510 (thrombospondin-1 analog) for the treatment of metastatic melanoma. *Am. J. Clin. Oncol.* **2007**, *30*, 303–309.
(50) Mochizuki, M.; Philp, D.; Hozumi, K.; Suzuki, N.; Yamada, Y.; Kleinman, H. K.; Nomizu, M. Angiogenic activity of syndecan-binding laminin peptide AG73 (RKRLQVQLSIRT). *Arch. Biochem. Biophys.* **2007**, *459*, 249–255.
(51) Hozumi, K.; Suzuki, N.; Nielsen, P. K.; Nomizu, M.; Yamada, Y. Laminin alpha1 chain LG4 module promotes cell attachment through syndecans and cell spreading through integrin alpha2beta1. *J. Biol. Chem.* **2006**, *281*, 32929–32940.
(52) Wickstrom, S. A.; Alitalo, K.; Keski-Oja, J. An endostatin-derived peptide interacts with integrins and regulates actin cytoskeleton and migration of endothelial cells. *J. Biol. Chem.* **2004**, *279*, 20178–20185.
(53) Mulder, W. J.; van der Schaft, D. W.; Hautvast, P. A.; Strijkers, G. J.; Koning, G. A.; Storm, G.; Mayo, K. H.; Griffioen, A. W.; Nicolay, K. Early in vivo assessment of angiostatic therapy efficacy by molecular MRI. *FASEB J.* **2007**, *21*, 378–383.
(54) de Lussanet, Q. G.; Beets-Tan, R. G.; Backes, W. H.; van der Schaft, D. W.; van Engelshoven, J. M.; Mayo, K. H.; Griffioen, A. W. Dynamic contrast-enhanced magnetic resonance imaging at 1.5 Tesla with gadopentetate dimeglumine to assess the angiostatic effects of anginex in mice. *Eur. J. Cancer* **2004**, *40*, 1262–1268.
(55) Brandwijk, R. J.; Mulder, W. J.; Nicolay, K.; Mayo, K. H.; Thijssen, V. L.; Griffioen, A. W. Anginex-conjugated liposomes for targeting of angiogenic endothelial cells. *Bioconjugate Chem.* **2007**, *18*, 785–790.
(56) Mayo, K. H.; Dings, R. P.; Flader, C.; Nesmelova, I.; Hargittai, B.; van der Schaft, D. W.; van Eijk, L. I.; Walek, D.; Haseman, J.; Hoye, T. R.; Griffioen, A. W. Design of a partial peptide mimetic of anginex with antiangiogenic and anticancer activity. *J. Biol. Chem.* **2003**, *278*, 45746–45752.
(57) Dings, R. P.; Arroyo, M. M.; Lockwood, N. A.; Van Eijk, L. I.; Haseman, J. R.; Griffioen, A. W.; Mayo, K. H. Beta-sheet is the bioactive conformation of the anti-angiogenic anginex peptide. *Biochem. J.* **2003**, *23*, 281–288.
(58) Kim, H. O.; Kahn, M. A merger of rational drug design and combinatorial chemistry: development and application of peptide secondary structure mimetics. *Comb. Chem. High Throughput Screening* **2000**, *3*, 167–183.
(59) Tsang, K. Y.; Diaz, H.; Graciani, N.; Kelly, J. W. Hydrophobic cluster formation is necessary for dibezofuran-based amino acids to function as β-sheet nucleators. *J. Am. Chem. Soc.* **1994**, *116*, 3988–4005.
(60) Blaskovich, M. A.; Lin, Q.; Delarue, F. L.; Sun, J.; Park, H. S.; Coppola, D.; Hamilton, A. D.; Sebti, S. M. Design of GFB-111, a platelet-derived growth factor binding molecule with antiangiogenic and anticancer activity against human tumors in mice. *Nat. Biotechnol.* **2000**, *18*, 1065–1070.
(61) Sun, J.; Blaskovich, M. A.; Jain, R. K.; Delarue, F.; Paris, D.; Brem, S.; Wotoczek-Obadia, M.; Lin, Q.; Coppola, D.; Choi, K.; Mullan, M.; Hamilton, A. D.; Sebti, S. M. Blocking angiogenesis and tumorigenesis with GFA-116, a synthetic molecule that inhibits binding of vascular endothelial growth factor to its receptor. *Cancer Res.* **2004**, *64*, 3586–3592.
(62) Sun, J.; Wang, D. A.; Jain, R. K.; Carie, A.; Paquette, S.; Ennis, E.; Blaskovich, M. A.; Baldini, L.; Coppola, D.; Hamilton, A. D.; Sebti, S. M. Inhibiting angiogenesis and tumorigenesis by a synthetic molecule that blocks binding of both VEGF and PDGF to their receptors. *Oncogene* **2005**, *24*, 4701–4709.
(63) Creighton, C. J.; Du, Y.; Santulli, R. J.; Tounge, B. A.; Reitz, A. B. Synthesis and biological evaluation of type VI beta-turn templated RGD peptidomimetics. *Bioorg. Med. Chem. Lett.* **2006**, *16*, 3971–3974.
(64) Athanassiou, Z.; Patora, K.; Dias, R. L.; Moehle, K.; Robinson, J. A.; Varani, G. Structure-guided peptidomimetic design leads to nanomolar beta-hairpin inhibitors of the Tat-TAR interaction of bovine immunodeficiency virus. *Biochemistry* **2007**, *46*, 741–751.
(65) Hammond, M. C.; Harris, B. Z.; Lim, W. A.; Bartlett, P. A. Beta strand peptidomimetics as potent PDZ domain ligands. *Chem. Biol.* **2006**, *13*, 1247–1251.
(66) Reichelt, A.; Martin, S. F. Synthesis and properties of cyclopropane-derived peptidomimetics. *Acc. Chem. Res.* **2006**, *39*, 433–442.
(67) Fu, Y.; Xu, B.; Zou, X.; Ma, C.; Yang, X.; Mou, K.; Fu, G.; Lu, Y.; Xu, P. Design and synthesis of a novel class of furan-based molecules as potential 20S proteasome inhibitors. *Bioorg. Med. Chem. Lett.* **2007**, *17*, 1102–1106.
(68) Dijkgraaf, I.; Kruijtzer, J. A.; Frielink, C.; Soede, A. C.; Hilbers, H. W.; Oyen, W. J.; Corstens, F. H.; Liskamp, R. M.; Boerman, O. C. Synthesis and biological evaluation of potent alphavbeta3-integrin receptor antagonists. *Nucl. Med. Biol.* **2006**, *33*, 953–961.
(69) Palomo, C.; Aizpurua, J. M.; Balentova, E.; Jimenez, A.; Oyarbide, J.; Fratila, R. M.; Miranda, J. I. Synthesis of beta-lactam scaffolds for ditopic peptidomimetics. *Org. Lett.* **2007**, *9*, 101–104.
(70) Baran, I.; Varekova, R. S.; Parthasarathi, L.; Suchomel, S.; Casey, F.; Shields, D. C. Identification of Potential Small Molecule Peptidomimetics Similar to Motifs in Proteins. *J. Chem. Inf. Model.,* in press.
(71) Berg, V.; Sellstedt, M.; Hedenstrom, M.; Pinkner, J. S.; Hultgren, S. J.; Almqvist, F. Design, synthesis and evaluation of peptidomimetics based on substituted bicyclic 2-pyridones-targeting virulence of uropathogenic E. coli. *Bioorg. Med. Chem.* **2006**, *14*, 7563–7581.
(72) Chen, X.; Dings, R. P.; Nesmelova, I.; Debbert, S.; Haseman, J. R.; Maxwell, J.; Hoye, T. R.; Mayo, K. H. Topomimetics of amphipathic beta-sheet and helix-forming bactericidal peptides neutralize lipopolysaccharide endotoxins. *J. Med. Chem.* **2006**, *49*, 7754–7765.
(73) Clore, G. M.; Appella, E.; Yamada, M.; Matsushima, K.; Gronenborn, A. M. Three-dimensional structure of interleukin 8 in solution. *Biochemistry* **1990**, *29*, 1689–1696.
(74) Gross, J. D.; Moerke, N. J.; von der Haar, T.; Lugovskoy, A. A.; Sachs, A. B.; McCarthy, J. E.; Wagner, G. Ribosome loading onto the mRNA cap is driven by conformational coupling between eIF4G and eIF4E. *Cell* **2003**, *115*, 739–750.

AR700086K